Mossbauer study of the 2212 phase of the bismuth superconductor

1993 J. Phys.: Condens. Matter 5 4541

(http://iopscience.iop.org/0953-8984/5/26/024)

J. Phys.: Condens. Matter 5 (1993) 4541–4556. Printed in the UK

Mossbauer study of the 2212 phase of the bismuth superconductor

S C Bhargava†, J S Chakrabarty†, H Jhans‡ and S K Malik‡

† Solid State Physics Division, Bhabha Atomic Research Centre, Bombay, 400 085, India

‡ Tata Institute of Fundamental Research, Colaba, Bombay, India

Received 10 November 1992, in final form 4 March 1993

Abstract. Mossbauer study of $Bi_2Sr_2CaCu_{2(1-x)}Fe_{2x}O_{8+d}$, $x \leqslant 0.12$, has been carried out. Samples have been characterized by x-ray, susceptibility and resistivity methods. Fe is expected to replace Cu. Even though, on average, all Cu sites are equivalent in this phase, each Mossbauer spectrum reveals at least two component spectra. The characteristics of the component spectra in the temperature range 4.2 K to 300 K and their dependences on x are determined. Possible origins of these components are discussed.

1. Introduction

Mossbauer spectroscopy has been used [1–16] to probe the high temperature oxide superconductors (HTSCs) by substituting Cu with Fe or Sn in places. A large number of research groups have made extensive investigations of Fe-doped $YBa_2Cu_3O_7$. This superconductor (SC), however, suffers from the disadvantage that only a small fraction of the probe Fe goes to the sites which form a part of the SC layer (Cu2 sites); by comparison, the 2212 phase of the bismuth cuprate superconductor has been considered ideal. Unlike in other phases, Cu in this oxide occupies square pyramidal sites only; this is known to be the prime configuration responsible for superconductivity in the oxide superconductors.

It is, however, well known that Fe has low preference for the Cu2 square pyramidal sites of $YBa_2Cu_3O_7$. Unlike other oxide superconductors, the 2212 phase does not present any other type of site to Fe. Consequently, there has been uncertainty as to whether Fe will occupy a sufficient number of square pyramidal sites of the 2212 phase of the bismuth superconductor or whether formation of other phases suitable for Fe occurs as a result of doping with Fe. Thus, the preparation of a single-phase sample of the Fe-doped 2212 Bi superconductor has been a challenging task.

Several routes have been followed to prepare the Fe-free 2212 phase of the Bi superconductor. The Pb-free phase obtained using the conventional solid state reaction method shows T_c lower than 85 K. Frequently, the transition shows a tail in the resistivity against temperature curve, which implies non-homogeneity and non-stoichiometry. A small amount of the 2201 or 2223 phase of the Bi superconductor also generally appears. Transition temperatures higher than 85 K have been reported using different procedures [17–20]. In the procedure followed here [20], $T_c(R = 0)$ of the Pb-free 2212 phase prepared in air is found to be 93 K. The temperature dependence of the resistivity is free from tails. No impurity phase was detectable using x-ray or neutron diffraction techniques. Using this procedure [20], Fe-doped samples of this phase have been made. Further heat treatments were found to be necessary to get good quality samples. The

0953-8984/93/264541+16$07.50

structural and magnetic properties of these Fe-doped samples have been studied using x-ray, susceptibility, EDAX and scanning electron microscopy (SEM). Mossbauer spectroscopy of $Bi_2Sr_2CaCu_{2(1-x)}Fe_{2x}O_{8+d}$, $x \leqslant 0.12$ has been performed in the temperature range 4.2 to 300 K, and thus x dependences of the hyperfine interaction parameters and site preferences and low-temperature measurements have been done for the first time. The low-temperature study aims to determine the nature of magnetic ordering, the possibility of the coexistence of magnetic order and superconductivity and the presence of spin relaxation effects in the Mossbauer magnetic spectra.

In earlier papers on Mossbauer investigations [10–16] of Bi superconductors the researchers have not discussed the characteristics of their samples in detail. In most cases impurity phases were detected with x-rays [10, 11, 13, 14]. Resistivity data are not presented except in [14]. In all cases, preparation of the samples was performed by the solid state reaction method. The procedures followed do not give special attention to the fact that Bi_2O_3 has a strong tendency to evaporate above 822 °C. Calcination has been done at temperatures as high as 850 °C [10–13]. It would therefore be interesting to know the stoichiometries and the superconducting behaviour of these samples. Bremert *et al* used a flowing oxygen atmosphere to prepare the sample [11]. Sintering in oxygen atmosphere can lead to a high intake of oxygen which not only leads to structural modulations but also to impurity phases. The amount of substitution made (20%) by Bremert *et al* is also large. As we will show here, large substitution results in the formation of impurity phases. Micklitz *et al* [12] studied the single-crystal and polycrystalline samples of Fe-doped 2212 phase made through different routes, yet the final compositions in the two cases are found to be similar. The Bi content of their samples is high in comparison to ours and may be responsible for the lower T_c obtained by them. The starting stoichiometries of the component oxides are not given; nor are the structural and superconducting characteristics. In the investigations by Lin *et al* [14], $T_c(R = 0)$ obtained was very low, 70 K, even for Fe-free samples. T_c decreased by 22 K for a Cu substitution of 3%. The transitions were found to be broad. Lin *et al* found that vacuum annealing improved the T_c of their samples substantially. This is not in agreement with our observations: we have found that T_c decreases when samples are annealed either in N_2 or in vacuum.

2. Experimental procedure

Bi_2O_3, $SrCO_3$, CuO, Fe_2O_3 and $CaCO_3$ of purities better than 99.9% are used to make the superconductors. The stoichiometric amounts of the oxides were taken. All of them, except Bi_2O_3, were mixed and heated at temperatures in the range 925 °C to 950 °C, depending on x, for 72 h, with two intermediate grindings. The temperature used was 930 °C for $x = 0.03$ and 0.06 and 950 °C for $x = 0.09$ and 0.12. Bi_2O_3 was subsequently added in the desired ratio and the mixture was melted for a moment and air quenched. This was then annealed at 850 °C for 16 h and quenched. This sample is labelled BSCC-A. Some of these samples were subsequently treated in N_2 at 750 °C for 8 h and slow cooled (99 °C per hour) or quenched; these samples are labelled BSCC-A,N. The other pellets of BSCC-A were not so treated. Both these types of pellet were further treated successively at 850, 855, 855 and 860 °C, for 16 h at each of these temperatures, followed by air quenching. These two types of pellet are designated BSCC-FN and BSCC-FA, respectively, depending on whether they were treated in N_2 earlier or not.

Mossbauer spectra at ambient temperature are obained using the spectrometer operated in constant acceleration mode. ^{57}Co in Rh is used as the source. Mossbauer spectra at

liquid helium temperature are obtained using a spectrometer operated with a sinusoidal drive waveform. Both ends of the long drive rod (≈ 1 m) are used to record spectra. The lower end, in the cold region of the liquid helium cryostat, carries the source for the oxide superconductor, while the upper end carries another source for calibration purposes. The Fe foil for calibration is kept outside the helium cryostat at the ambient temperature. Both spectra are recorded simultaneously by a control and data acquisition system connected to an IBM personal computer. The velocity scale of the spectra is linearized after the analyses, for display purposes only. The spectrometer provides a calibration spectrum for Fe metal with lines of width ≈ 0.23 mm s^{-1}. Resistivity measurements are made using the DC four-probe method.

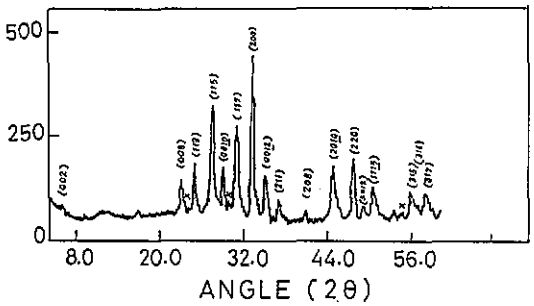

Figure 1. The x-ray diffraction pattern of a BSCC-FN sample of $Bi_2Sr_2CaCu_{2(1-x)}Fe_{2x}O_{8+d}$, $x = 0.03$.

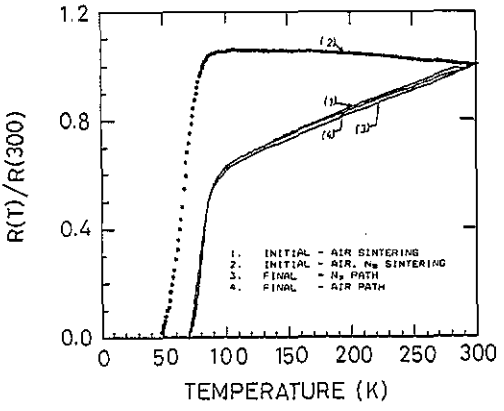

Figure 2. The temperature dependences of the resistivities of the four samples BSCC-A, BSCC-A,N, BSCC-FA and BSCC-FN of $Bi_2Sr_2CaCu_{2(1-x)}Fe_{2x}O_{8+d}$, $x = 0.03$.

Table 1. The results of analyses of the Mossbauer spectra of the four samples of $Bi_2Sr_2CaCu_{2(1-x)}Fe_{2x}O_{8+d}$, $x = 0.03$: BSCC-A, BSCC-A,N, BSCC-FA and BSCC-FN, using two doublets as well as three doublets. Two sets of parameters obtained using three symmetric doublets which fit the spectra equally well are given.

	Component 1			Component 2			Component 3		
Sample	QS (mm s^{-1})	IS* (mm s^{-1})	I (%)	QS (mm s^{-1})	IS* (mm s^{-1})	I (%)	QS (mm s^{-1})	IS* (mm s^{-1})	I (%)
3%-A	0.69	0.23	33	1.77	0.245	67			
	0.68	0.24	36	1.80	0.13	23	1.76	0.33	41
	0.665	0.24	34	2.01	0.24	22	1.61	0.26	44
3%-A,N	0.63	0.22	19	1.68	0.23	81			
3%-FA	0.64	0.24	27	1.725	0.23	73			
	0.63	0.245	31	1.78	0.13	36	1.68	0.35	33
	0.62	0.24	29	1.99	0.11	23	1.565	0.25	48
3%-FN	0.67	0.25	33	1.74	0.24	67			
	0.66	0.25	36	1.96	0.23	30	1.55	0.26	34
	0.67	0.25	36	1.785	0.12	24	1.72	0.32	40

* Isomer shift with respect to Fe metal.

3. Results

3.1. $Bi_2Sr_2CaCu_{2(1-x)}Fe_{2x}O_{8+d}$, $x = 0.03$

X-ray diffraction patterns of 3%-A, 3%-A,N, 3%-FA and 3%-FN samples are similar (figure 1). No impurity phase was detected. The temperature dependences of the resistivities of the four samples are shown in figure 2. T_c of BSCC-A,N is lower than T_c of other samples by ≈ 20 K. The Mossbauer spectrum of any of these samples shows the presence of two component spectra (figure 3). The fit of the spectrum of BSCC-FN using two doublets is shown in figure 3. The results are given in table 1. In some of the earlier studies, three components have been used to fit the spectrum. Our analyses show that it is possible to get two different sets of parameters for the three symmetric doublets and get equally good fits. Both these sets are included in table 1. The corresponding fits are also shown in figure 3.

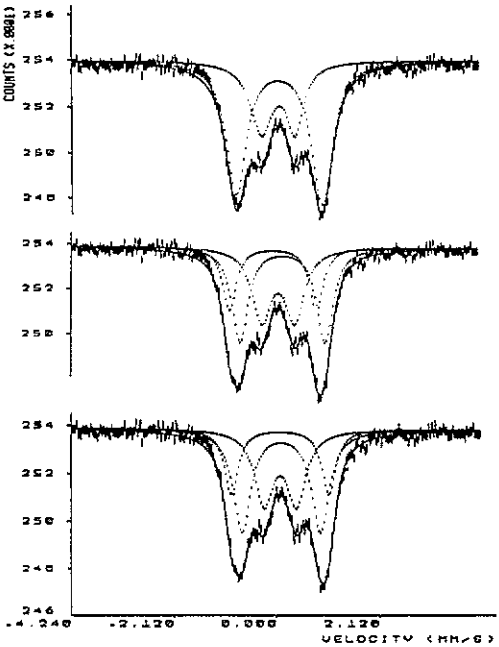

Figure 3. The Mossbauer spectrum of $Bi_2Sr_2CaCu_{2(1-x)}Fe_{2x}O_{8+d}$, $x = 0.03$ (BSCC-FN), at 300 K. The fits of the experimental data using two and three doublets are shown by full curves. The component spectra are shown by dotted curves.

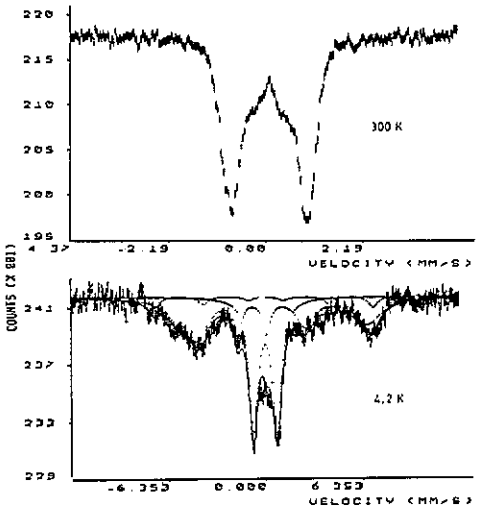

Figure 4. The Mossbauer spectra of $Bi_2Sr_2CaCu_{2(1-x)}Fe_{2x}O_{8+d}$, $x = 0.03$ (BSCC-A,N) at 300 and 4.2 K. The fit of the spectrum at 4.2 K obtained using two sextets and a symmetric paramagnetic doublet is shown by a full curve along with the component theoretical spectra.

The spectrum of BSCC-A,N differs from other spectra in an interesting way. The relative intensity of the inner doublet is lower than in other spectra. We have chosen this sample for the study at lower temperatures so the characteristics of the outer component at lower temperatures can be determined more precisely. The spectrum at 4.2 K (figure 4) consists of a paramagnetic as well as two magnetic component spectra. We assumed that the corresponding lines in a sextet have equal linewidths and depths. The relative intensities of the three pairs of lines are assumed to be 3:2:1. The two lines of the doublet are also assumed to be symmetric. The results are given in table 2. The fit in the outer parts of the

spectrum is unique and provides hyperfine magnetic fields, electric quadrupole shifts and isomer shifts characterizing the two magnetic sextets accurately. The line overlap is large in the innermost part of the spectrum. The fit in this part is therefore not unique; it is highly dependent on the constraints used. We use the reasonable constraint that the inner lines of a sextet are three times less intense than the outermost lines. Nevertheless, the accuracy of the parameters characterizing the paramagnetic component thus obtained is limited.

Table 2. Result of analyses of the Mossbauer spectra of $Bi_2Sr_2CaCu_{2(1-x)}Fe_{2x}O_{8+d}$, $x = 0.03$ and 0.06, at 4.2 K.

Composition x	Component No	H_{INT} (kG)	IS (mm s^{-1})	$(\delta_{12} - \delta_{56})$ (mm s^{-1})
0.03	1	443 ± 2.5	0.32	0.25
	2	373 ± 2	0.115	3.07
	3	——	0.32	1.50
0.06	1	421 ± 1.5	0.29	0.79
	2	367 ± 3	0.25	1.95
	3	——	0.13	1.30

3.2. $Bi_2Sr_2CaCu_{2(1-x)}Fe_{2x}O_{8+d}$, $x = 0.06$

Samples of 6%-A, 6%-FN and 6%-FA have been studied. The T_c values of BSSC-A, BSSC-FA and BSSC-FN samples are not significantly different (figure 5). The T_c of BSCC-A,N is, however, distinctly lower and shows less metallic behaviour in the normal state. The x-ray diffraction patterns of these samples do not show significant differences and the impurity-phase contents of the samples are negligible (figure 6). SEM spectra of BSCC-FA and BSCC-FN samples are shown in figure 7. The pellet is broken into two pieces and the micrograph of the transverse section is taken. EDAX shows the chemical composition of the BSCC-FN sample to be $Bi_{1.60}Sr_{2.00}Ca_{0.99}Cu_{1.88}Fe_{0.12}O_z$. Mossbauer spectra of any of the three samples show the presence of two doublets. A least-squares fit to the spectra using two doublets gives results as shown in table 3. As in the case of the spectra of the sample with 3% substitution, it is possible to fit these spectra with three doublets. The two sets of parameters obtained are also given in table 3. The fit obtained using the three doublets is better (figure 8). The spectrum at 4.2 K (figure 9) consists of a paramagnetic as well as two magnetic components, similar to the spectra of the sample with $x = 0.03$ at 4.2 K. It is fitted with two sextets and a doublet. We assumed that the corresponding lines in a sextet have equal linewidths and depths. The relative intensities of the three pairs of lines are assumed to be 3:2:1. The two lines of the doublet are also assumed to be symmetric. The results are included in table 2.

3.3. $Bi_2Sr_2CaCu_{2(1-x)}Fe_{2x}O_{8+d}$, $x = 0.09$

The x-ray diffraction pattern of BSCC-A shows the presence of a small amount of an impurity phase, whose concentration decreases with subsequent heat treatment. The peaks of the impurity phase have been marked with crosses in figure 10. The sample was further heat treated to prepare BSCC-FN and BSCC-FA. X-ray diffraction patterns of the two samples (BSCC-FA and BSCC-FN) are similar. Impurity peaks are negligible. The lines are also narrower showing better crystallinity of BSCC-FA and BSCC-FN. Thus, the subsequent heat treatments are helpful in removing the impurity phase and improving crystallinity.

Resistivity measurements show changes in T_c due to the heat treatments as shown in figure 11. The width of the SC transition increases with x, to approximately 30 K in the

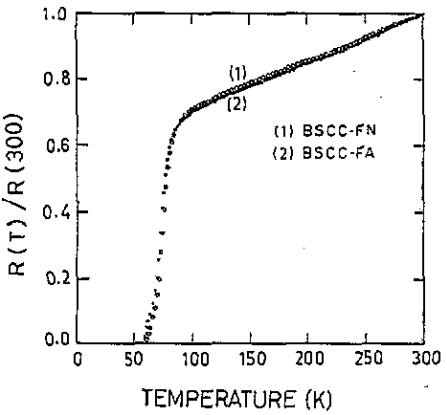

Figure 5. The temperature dependences of the resistivities of the three samples BSCC-A, BSCC-FA and BSSC-FN of $Bi_2Sr_2CaCu_{2(1-x)}Fe_{2x}O_{8+d}$, $x = 0.06$.

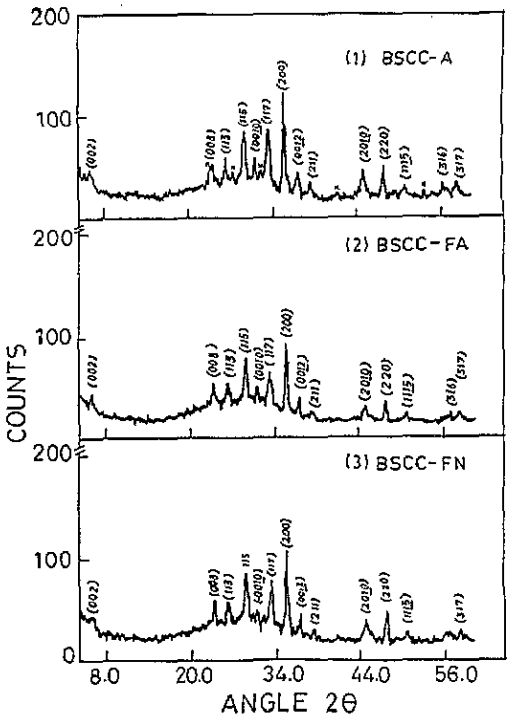

Figure 6. The x-ray diffraction pattern of $Bi_2Sr_2CaCu_{2(1-x)}Fe_{2x}O_{8+d}$, $x = 0.06$.

present case. $T_c(R = 0)$ also drops to 48 K. The treatment in N_2 (BSCC-A,N) decreases T_c, decreases the metallic nature of the oxide and broadens the SC transition further. This is found in samples with other values of x too, and appears to be due to a decrease in the oxygen content of the sample. This interpretation is confirmed by treating the sample in vacuum at 500 °C, which not only decreases T_c drastically but also increases the semiconducting nature of the oxide further.

Mossbauer spectra of BSCC-A, BSCC-FA and BSCC-FN are shown in figure 12. They are fitted with two symmetric doublets. The results are given in table 4. The relative intensity of the inner doublet is larger in BSCCA-FA and BSCC-FN than in BSCC-A. The relative intensity of the inner doublet of BSCC-A increases with time and tends to become equal to its relative intensity in BSCC-FN,FA. Thus, the relative distributions of Fe at the two sites acquire stable values after all the heat treatments

3.4. $Bi_2Sr_2CaCu_{2(1-x)}Fe_{2x}O_{8+d}$, $x = 0.12$

The BSCC-A sample of this composition shows the presence of a significant amount of impurity phase (figure 13). On the other hand, the impurity peaks in x-ray patterns of BSCC-FA,FN are small, though not negligible. The peaks of the impurity phase have been marked with crosses in figure 13.

BSCC-A is metallic in the normal state and has a $T_c(R = 0)$ of 50 K (figure 14). BSCC-FA and BSCC-FN, on the other hand, are semiconducting in the normal state and have broader SC transitions. The values of $T_c(R = 0)$ are 30 K, but T_c onsets are not significantly lower than that of BSCC-A. Thus it appears that the subsequent treatment has resulted in a higher

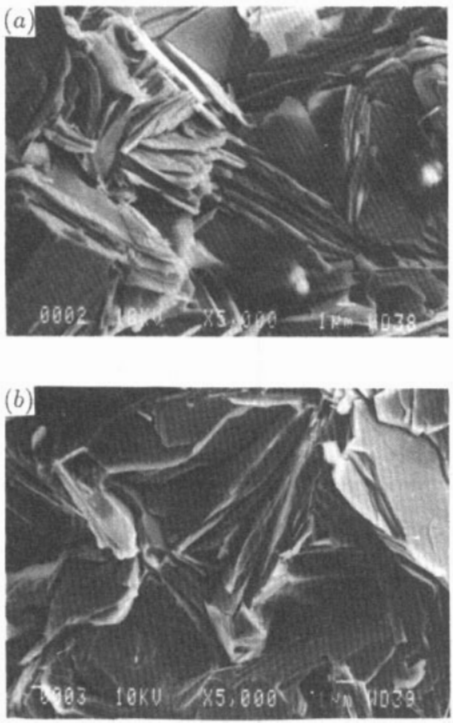

Figure 7. Scanning electron micrographs of $Bi_2Sr_2CaCu_{2(1-x)}Fe_{2x}O_{8+d}$, $x = 0.06$: (*a*) BSCC-FN and (*b*) BSSC-FA. The pellet was broken into two pieces and the area along the thickness examined.

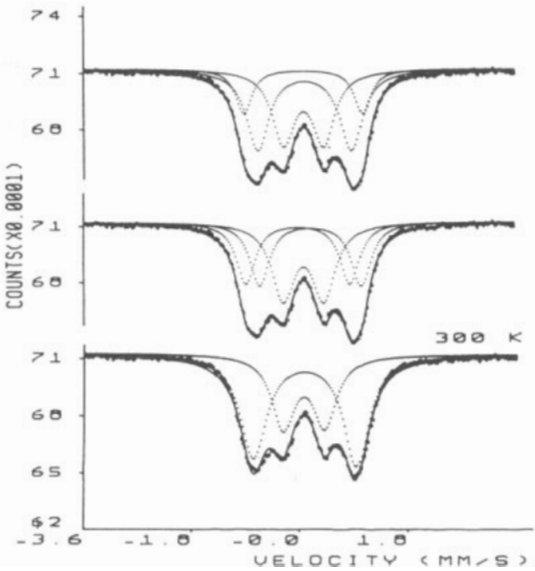

Figure 8. Mossbauer spectra of $Bi_2Sr_2CaCu_{2(1-x)}Fe_{2x}O_{8+d}$, $x = 0.06$ (BSCC-FN). The fits of the experimental data using two and three doublets are shown by full curves. The component spectra are shown by dotted curves.

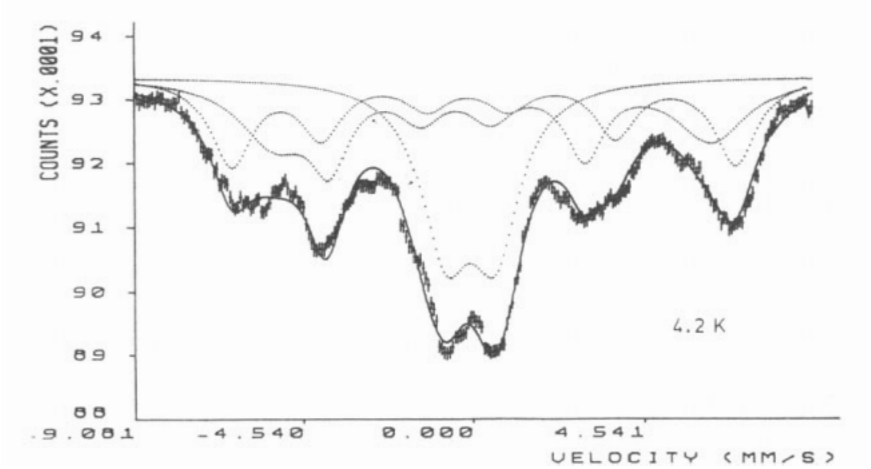

Figure 9. Mossbauer spectrum of $Bi_2Sr_2CaCu_{2(1-x)}Fe_{2x}O_{8+d}$, $x = 0.06$ (BSCC-FN) at 4.2 K. The fit obtained using two sextets and a symmetric paramagnetic doublet is shown by a full curve along with the component theoretical spectra.

Table 3. The results of analyses of the Mossbauer spectra of the three samples of $Bi_2Sr_2CaCu_{2(1-x)}Fe_{2x})_{8+d}$, $x = 0.06$: BSCC-A, BSCC-FA, BSCC-FN, using two doublets as well as three doublets. Two sets of parameters obtained using three symmetric doublets which fit the spectra equally well are given.

	Component 1			Component 2			Component 3		
Sample	QS (mm s^{-1})	IS* (mm s^{-1})	I (%)	QS (mm s^{-1})	IS* (mm s^{-1})	I (%)	QS (mm s^{-1})	IS* (mm s^{-1})	I (%)
6%-A	0.69	0.24	44	1.70	0.20	56			
(173 K)	0.73	0.23	38	1.79	0.10	31	1.75	0.33	31
	0.72	0.23	35	2.02	0.115	24	1.57	0.22	41
6%-FA	0.74	0.23	45	1.83	0.22	55			
(300 K)	0.72	0.24	46	1.85	0.11	23	1.795	0.33	31
	0.70	0.24	42	2.03	0.21	24	1.58	0.24	34
6%-FN	0.68	0.22	36	1.705	0.23	64			
(330 K)	0.67	0.22	38	1.98	0.21	18	1.56	0.23	44
	0.68	0.22	41	1.69	0.33	30	1.74	0.12	29

* Isomer shift with respect to Fe metal.

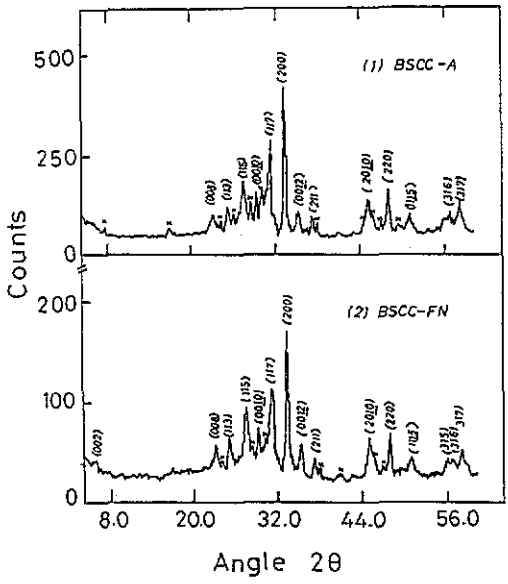

Figure 10. The x-ray diffraction pattern of $Bi_2Sr_2CaCu_{2(1-x)}Fe_{2x}O_{8+d}$, $x = 0.09$.

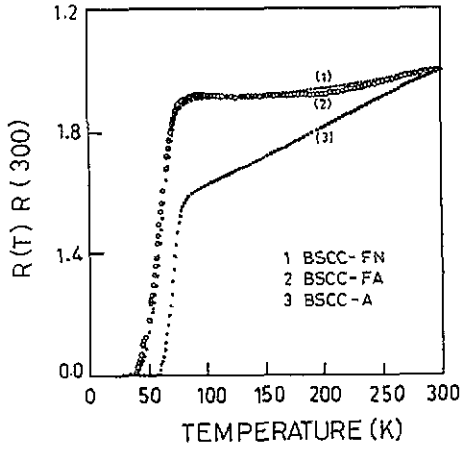

Figure 11. Temperature dependences of the resistivities of the three samples BSCC-A, BSCC-FA and BSCC-FN of $Bi_2Sr_2CaCu_{2(1-x)}Fe_{2x}O_{8+d}$, $x = 0.09$.

content of Fe in the SC lattice in BSCC-FA and BSCC-FN than in BSCC-A. No appreciable tail in the R against T curve is visible. The AC susceptibility, χ_{AC}, of BSCC-FN and BSCC-FA pellets show the onset of bulk superconductivity at ≈ 30 K, in agreement with $T_c(R = 0)$ of BSCC-FA and BSCC-FN (figure 15).

The Mossbauer spectrum at ambient temperature has been split into two symmetric doublets. The fitted spectra are shown in figure 16 and the results included in table 4. Thus, the formation of the impurity phase has not resulted in the appearance of any extra component in the Mossbauer spectrum. This implies that the impurity phase does not contain Fe. It is also unlikely that one of the two Mossbauer components corresponds to this impurity

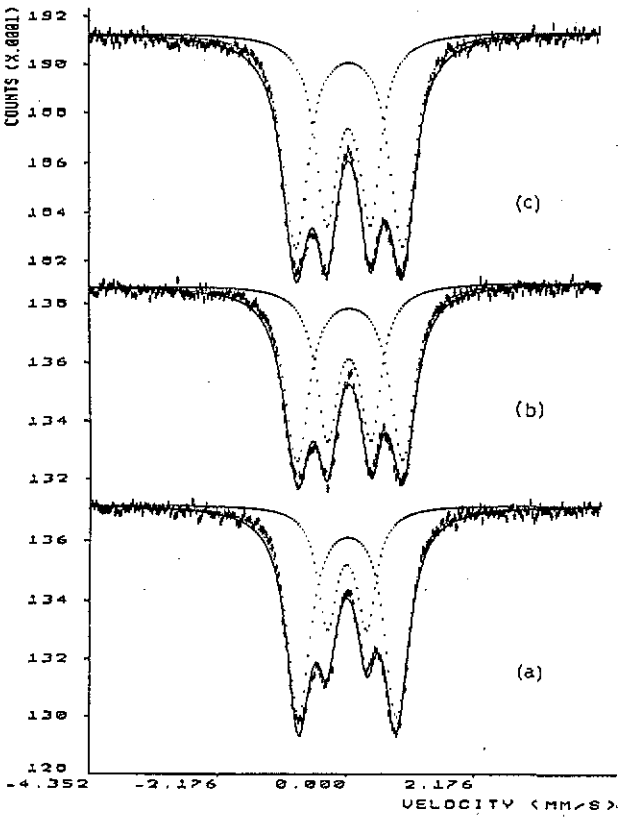

Figure 12. Mossbauer spectra of the three samples of $Bi_2Sr_2CaCu_{2(1-x)}Fe_{2x}O_{8+d}$, $x = 0.09$: (*a*) BSCC-A, (*b*) BSSC-FN and (*c*) BSSC-FA. The curves which fit best are drawn as full curves.

Table 4. The results of analyses of the Mossbauer spectra of the three samples of $Bi_2Sr_2CaCu_{2(1-x)}Fe_{2x}O_{8+d}$, $x = 0.09$ (BSCC-A, BSCC-FA, BSCC-FN), and two samples of $Bi_2Sr_2CaCu_{2(1-x)}Fe_{2x}O_{8+d}$, $x = 0.12$, BSCC-FA and BSCC-FN, using two doublets.

	Component 1			Component 2		
Sample	QS (mm s^{-1})	IS* (mm s^{-1})	I (%)	QS (mm s^{-1})	IS* (mm s^{-1})	I (%)
9%-A	0.66	0.21	31	1.65	0.23	69
9%-FA	0.73	0.24	43	1.79	0.25	57
9%-FN	0.73	0.24	42	1.78	0.25	58
12%-FA	0.78	0.23	51	1.82	0.25	49
12%-FN	0.78	0.24	50	1.84	0.25	50

* Isomer shift with respect to Fe metal.

phase, because in the sample with lower x both Mossbauer components are large in relative intensity even though the impurity phase is not shown by x-rays. Furthermore, the impurity phase appears to be non-superconductive because its presence has not resulted in a tail in the R against T curve.

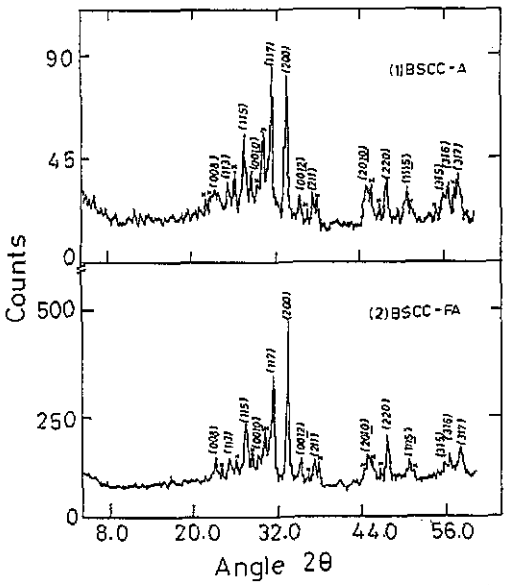

Figure 13. The x-ray diffraction pattern of $Bi_2Sr_2CaCu_{2(1-x)}Fe_{2x}O_{8+d}$, $x = 0.12$. The diffraction patterns of BSCC-FA and BSCC-FN are similar.

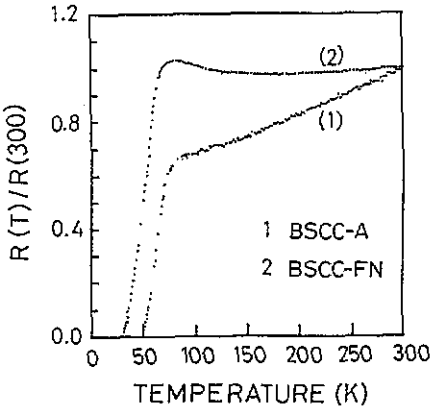

Figure 14. The temperature dependences of the resistivities of the two samples BSCC-A and BSCC-FN of $Bi_2Sr_2CaCu_{2(1-x)}Fe_{2x}O_{8+d}$, $x = 0.12$. The dependences of BSCC-FA and BSCC-FN are not appreciably different.

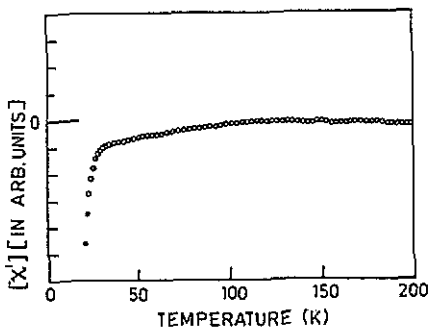

Figure 15. χ_{AC} of $Bi_2Sr_2CaCu_{2(1-x)}Fe_{2x}O_{8+d}$, $x = 0.12$ (BSCC-FN). The frequency used is 313 Hz and the field is about 0.5 G.

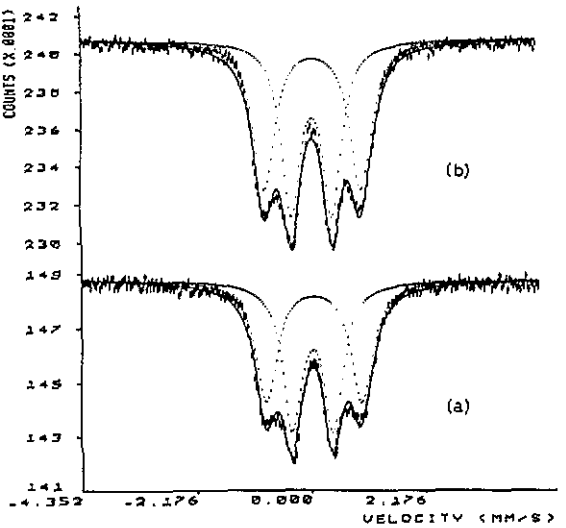

Figure 16. Mossbauer spectra of the two samples of $Bi_2Sr_2CaCu_{2(1-x)}Fe_{2x}O_{8+d}$, $x = 0.12$: (*a*) BSCC-FA and (*b*) BSCC-FN. The best fits are drawn as full curves. The component spectra are shown by dotted curves.

4. Discussion

4.1. Fe occupies Cu sites

On average, all Cu sites in the 2212 phase of the Bi superconductor are equivalent. However, the number of component spectra in the Mossbauer spectrum is certainly greater than one. The possibility that Fe substitutes for other cations has also been ruled out in earlier studies. A large number of investigations have shown that Fe, Co, Mn, Zn, etc substitute at Cu sites only, and significantly reduce T_c and the metallic nature of high-temperature superconductors [1–16, 21–35]. Such studies are abundant for the case of $YBa_2Cu_3O_7$ [21–30] because of the ease with which this superconductor can be prepared. Thus, neutron and electron diffraction [21–25], EXAFS [26–29], anomalous x-ray scattering [30], and Mossbauer spectroscopy [1–3] have shown that Fe atoms substitute for Cu atoms in $YBa_2Cu_3O_7$ only. The change in superconducting properties is gradual as the concentration of the dopant is increased. The Mossbauer spectrum is also characteristic of the dopant and oxygen ion concentrations in the oxide. Indeed, by observing all of these it is possible to ascertain whether Fe has occupied the desired Cu site in $YBa_2Cu_3O_7$. The effects of the substitution and the site preferences of Fe, Co, Zn, Ni, etc in $Bi_2Sr_2CaCu_2O_{8+d}$ have also been studied [10–16, 31–35]. These ions are found to substitute for Cu only.

4.2. The cause of two doublets

In an interesting experiment, Tarascon *et al* [5] have shown that superstructural modulations present in the Bi superconductor result in more than one component spectrum even when all Cu sites in the lattice are equivalent. $Bi_{2-x}Pb_xSr_2MO_y$ (M=Mn, Co, Fe) centred around $x = 1$ are isostructural to the 2201 phase of the bismuth cuprate with $T_c \approx 10$ K, but lack the structural modulation present in $Bi_2Sr_2CuO_6$ (2201 Pb-free phase). In this PbBi phase, i.e. 50% of Bi replaced by Pb, full substitution of Cu by Fe can be achieved. On the other hand, in the 2201 Pb-free phase, the substitution of Cu by Fe is limited to 50%. Mossbauer spectra of $Bi_2Sr_2Cu_{0.6}Fe_{0.4}O_y$, in which the structural modulations are present, show the presence of two doublets with splittings of 1.64 and 0.65 and isomer shifts of 0.22 and 0.18 mm s^{-1}, respectively. Mossbauer spectra of $PbBiSr_2FeO_y$, which has a non-modulated structure, show only one doublet with electric quadrupole splitting (EQS) of 1.48 mm s^{-1}. However, lines are broad ($\Gamma \approx 0.5$ mm s^{-1}) even without modulation. Thus, the appearance of superstructural modulation is responsible for the appearance of more than one doublet but the line broadening is present even without modulation.

Superstructure modulations result from extra O rows in the Bi layers. The excess O can occupy the CaO layer in the vicinity of Fe at the Cu sites, because Fe has strong preference for the octahedral coordination. The larger intake of O at higher Fe concentration, beyond that required for superstructural modulation, has been experimentally confirmed. Thus, there are two ways in which the excess O can affect the spectrum: either through the direct effect of the superstructural modulation in the BiO layer, or through the insertion of extra O into the CaO layer, close to Fe. The latter is far more effective in changing the hyperfine interaction parameters and is more likely in view of the large differences observed in the parameters characterizing the two doublets. Of course, in both cases, superstructural modulation are present.

A few other characteristics of the inner doublet need to be considered: (i) the relative intensity of the inner doublet in the spectrum of BSCC-A increases with time and tends to become equal to the value found in the spectrum of BSCC-FA,FN; (ii) the relative intensity of the inner doublet in the BSCC-A spectrum increases with the further heat treatment which

leads to BSCC-FA, and BSCC-FN; (iii) the relative intensity of the inner doublet increases as the concentration of Fe increases; (iv) the relative intensity of the inner doublet is smaller in the single-crystal sample than in the polycrystalline sample [12]; (v) this component is found in the spectra of all high-temperature superconductors; (vi) its isomer shift is always distinctly characteristic of Fe^{3+}; (vii) it always shows saturation hyperfine magnetic field $\geqslant 425$ kG when magnetically split, which shows that these Fe^{3+} ions are in high-spin states in all cases; (viii) the quadrupole shift in the magnetic spectra shows that spins lie in the *ab* plane in all cases if it is assumed that V_{zz} is along the *c*-axis and is axial.

This inner component is believed to result from the Fe atoms at the square pyramidal Cu2 sites in $YBa_2Cu_3O_7$, but the origin of this component in the case of $Bi_2Sr_2CaCu_2O_8$ is not considered to be Fe at the Cu sites with square-pyramid oxygen coordination. No evidence was presented, however, for this interpretation in the case of the Bi superconductor [10–16].

It appears that in the air-quenched sample of BSSC-A, a stable structure is not obtained even though the x-ray diffraction pattern shows the formation of the superconductor lattice. With the passage of time or on further heat treatment the stable structure is obtained, which leads to improved crystallinity, indicated by the narrowing of the x-ray lines and the increase in the relative intensity of the inner Mossbauer doublet. This, in turn, results from the appearance of structural modulation. Thus, the modulations are stabilized with further heat treatment or with the passage of time. The fact that the stable structure is not obtained initially may be due to the air quenching used to cool the sample from 850 °C. The transormation to a stable structure may be due to atomic movement on a microscopic scale, or to migration or the intake of oxygen ions. The strong tendency to acquire stable structure makes this change possible even at ambient temperature.

4.3. Number of component spectra

Barb *et al* [10], Micklitz *et al* [12] and Morrish *et al* [9] have fitted the Mossbauer spectra of the 2212 phase with two doublets only. In other investigations three doublets have been used. There is no unambiguous evidence available, however, from earlier studies to support a fit with three doublets. The parameters characterizing the component spectra of 2212, 2201 and 2223 phases are not much different. Thus, if the 2201 or 2223 phase is present along with the 2212 phase, a fit using three overlapping doublets would be desirable. In the study by Lin *et al* [14], the solid state reaction method, which is known to give the 2201 phase too, is used to prepare the sample. The T_c obtained is low and the superconducting transition is wide. Thus, a fit by three doublets is reasonable. In the case of Bremert *et al* [11], the concentration of the dopant used is very high (20%). The formation of an impurity phase is expected and thus a fit to three doublets is understandable. In the samples prepared by Tittonen *et al* [13], impurity phases are also present, and the spectra have been fitted with three doublets.

The line broadening indicates a spread in the values of electric field gradient (EFG) and isomer shift which characterize the component spectra. Its origin is not clear at this stage. The possibility of superstructural modulations causing the line broadening was ruled out by Tarascon *et al* [5]. The fit to the broad spectrum improves, particularly in the outer parts, as the number of components used to fit the spectrum is increased. No additional information is, however, available from such an exercise except to confirm that there is a spread in the values of EFG and isomer shifts. We preferred to use only two doublets to fit the spectra. In some cases, we also fit the data with three doublets. Two quite different sets of parameters for the three doublets were found to fit the experimental spectrum equally well, which clearly shows non-uniqueness.

4.4. Magnitude of EFG and isomer shifts

Another interesting result pointed out by Micklitz *et al* [12] is that the Cu nuclear quadrupole resonance (NQR) frequencies at the square pyramidal sites of $YBa_2Cu_3O_7$ and $Bi_2Sr_2CaCu_2O_8$ are same [36, 37]. Consequently, the hyperfine interaction parameters of Fe at these two sites must be similar if the ionic states of Fe in the two cases are the same. In earlier studies, the doublet with splitting ≈ 1.7 mm s^{-1} in the spectrum of the 2212 phase and the doublet with splitting ≈ 0.67 mm s^{-1} in the spectrum of $YBa_2Cu_3O_7$ were assigned to Fe with square pyramid coordination of oxygen ions. The isomer shifts of these two doublets are characteristic of the same charge state, Fe^{3+}. Thus, the difference in the magnitudes of quadrupole shifts and hyperfine magnetic fields is possible if the spin states are different in the two cases. In the following we examine this possibility.

The splitting of the d state in fields of various symmetries is shown schematically in figure 17. In an octahedral field, the fivefold degenerate level splits into a ground triplet ($|xy\rangle$, $|xz\rangle$, and $|yz\rangle$) and the excited doublet ($|z^2\rangle$ and $|x^2 - y^2\rangle$). In the case of tetragonal distortion, obtained by the displacement of ions along the z-axis away from the centre, the excited state splits into two states and the ground state into a doublet and a singlet. These splittings increase as the square pyramid coordination is approached. Finally, when the other ion along the z-axis is also removed to infinity to obtain the square planar configurations, these splittings reach a maximum. A discussion of these aspects can be found in [38] or in any crystal field theory text. The possibility of the ionic state becoming a low-spin state, with $S = 3/2$, increases as these splittings increase. Hund's rule is followed as long as crystal field splitting is smaller than E_H ($\approx 30\,000$ cm^{-1}). The crystal field splitting (10 Dq) in the field of octahedral symmetry $\approx 14\,000$ cm^{-1} for Fe^{3+} [38]. Thus, in this case, Hund's rule is followed and results in a high-spin Fe^{3+} ion with $S = 5/2$. In this case, the valence contribution to EFG is zero. The lattice contribution is also small for a predominantly octahedral environment. Consequently, the EQS is expected to be small. The hyperfine magnetic field is expected to be close to 500 kG. On the other hand, when the energy splitting between the lowest level and the excited $|x^2 - z^2\rangle$ state becomes large due to a change from octahedral to square pyramidal coordination, we can get a low-spin configuration of Fe^{3+} with $S = 3/2$. In this case, the valence electrons as well as the lattice charges make an appreciable contribution to the EFG. EQS is expected to be large. The hyperfine field is also ≈ 330 kG.

For the ion to be in a high-spin state at the Cu2 site in $YBa_2Cu_3O_7$ and in a low-spin state at the square pyramid Cu site in $Bi_2Sr_2CaCu_2O_8$, we should have apical O relatively farther from the Fe ion in the Bi superconductor. We give the relevant Cu–O distances in table 5, which clearly rule out the possibility of different spin states of Fe^{3+} in the two cases. Consequently, the assignment of widely differing Mossbauer components to Fe at the square pyramidal sites in $Bi_2Sr_2CaCu_2O_8$ and $YBa_2Cu_3O_7$ is not in agreement with NQR results as well as crystal field considerations. It is, however, accepted that the assignment in the case of $YBa_2Cu_3O_7$ is correct. Consequently, we must assume that the inner component in the spectrum of $Bi_2Sr_2CaCu_2O_8$ corresponds to Fe atoms on the square pyramid sites. However, in this case the origin of the outer component is not clear.

A similar anomalous observation [5] is the large splitting of the doublet in the spectrum of $PbBiSr_2FeO_6$ (≈ 1.48 mm s^{-1}) even though Fe sites are octahedrally coordinated to oxygen ions with slight tetragonal elongation of the oxygen ions along the z-axis.

4.5. Magnetic spectra

The spectrum at 4.2 K shows the coexistence of magnetic and paramagnetic components. Line widths in the magnetic spectra are large and can be caused by a distribution in hyperfine

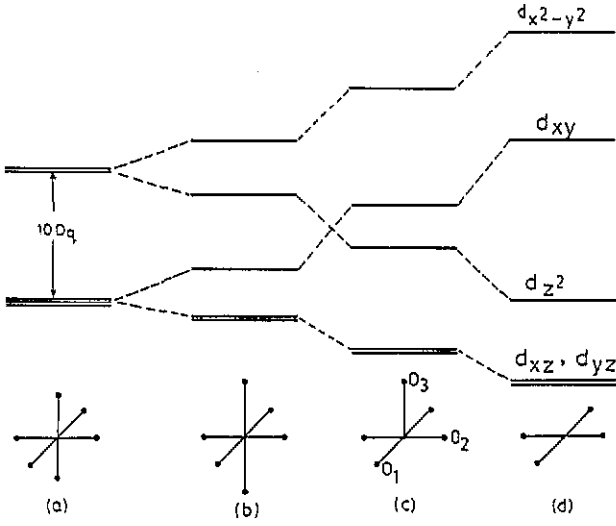

Figure 17. Schematic representation of d-level splitting in fields of various symmetries.

Table 5. Cu–O ion distances in the square pyramid coordination of Cu ions in $YBa_2Cu_3O_7$ and $Bi_2Sr_2CaCu_2O_8$ (see figure 17).

Superconductor	Cu–O_1 (×2) (Å)	Cu–O_1(×2) (Å)	Cu–O_3(×1) (Å)	Ref.
$Bi_2Sr_2CaCu_2O_8$	1.99	1.88	2.26	[39]
	1.93–1.94	1.88	2.38–2.58	[41]
$YBa_2Cu_3O_7$	1.927	1.961	2.301	[40]

interaction parameters as a result of structural variations. Another intrinsic mechanism, as in the case of broadening of the paramagnetic component, cannot be ruled out at this stage. The alternative possibility is the presence of relaxation effects which not only broaden the lines but also affect line positions. As the relaxation frequency increases, the lines start moving towards the centre; the inner lines are the first to move in. The values of δ_{16}/δ_{34} and δ_{25}/δ_{34} in a sextet are 6.327 and 3.663, respectively, in the absence of relaxation. Here, δ_{ij} denotes the separation between the ith and jth lines of a sextet. As the relaxation frequency increases, these ratios start increasing due to the preferential inward motion of the inner pair of lines. Subsequently, outer lines also move in. Only when the relaxation frequency becomes very large do the ratios regain their static values and relaxation effects disappear. This is generally the case in the spectra of magnetic substances. We have, however, successfully fitted the spectra at 4.2 K by keeping the values of these parameters as 6.327 and 3.663, respectively. The fit obtained is satisfactory. Furthermore, in the presence of relaxation, linewidths, δ_{16}/δ_{34} and δ_{25}/δ_{34} increase with temperature. This has not been found in the temperature range in which the magnetic splitting appears, i.e. from 4.2 to 15 K. Thus, unlike in the case of $YBa_2Cu_3O_7$, we have not found evidence of spin relaxation effects on the magnetic hyperfine spectra of the Bi superconductor. This implies that magnetic ordering and superconductivity coexist in the present case. This, however, does not contradict the results obtained using BCS superconductors, in which magnetic impurity destroyed superconductivity, if the magnetic ordering of Fe in the Bi superconductor is of spin glass type [42, 43]. The magnetic correlation length in this case can be smaller than the superconducting coherence length. It has been shown by the neutron diffraction method [42, 43] that the magnetic ordering of Fe at low temperatures is indeed

characteristic of spin glass.

The coexistence of the paramagnetic component and the two magnetic components can also be explained as being due to spin glass behaviour or superparamagnetism. Earlier studies have shown that whereas the spin glass freezing in the metallic substances occurs sharply at some temperature, this is not so in oxide spin glasses. This is due to the long-range and short-range nature of magnetic interactions in metallic and non-metallic substances, respectively. As a result, spins in oxides progressively freeze as the temperature is lowered. The short-range nature of the magnetic interactions in oxides also frequently leads to superparamagnetism when the concentration of magnetic ions is low. As a result of either or both of these, in a certain range of temperature, the paramagnetic component coexists with the magnetic spectrum. The intensity of the paramagnetic component decreases and that of the magnetic component increases as more and more spins freeze due to the lowering of temperature. However, unlike the conventional spin glass oxides, the oxides under study are high-temperature superconductors. The effect of the presence of superconductivity on the characteristic differences in the behaviour of metallic and non-metallic spin glasses is not clear. The coexistence of magnetic and paramagnetic components has also been found in the spectra of Fe in the 2223 phase of the Bi superconductor [8] and $Bi_2Sr_2YCu_2O_{8+d}$ [16] at low temperatures.

5. Conclusions

Fe can replace Cu in $Bi_2Sr_2CaCu_2O_8$ up to 8% without forming an impurity phase. T_c decreases by 4.8 K for 1% substitution, linearly up to 8%. Fe occupies Cu sites only. Two doublets are observed in the paramagnetic Mossbauer spectra, even though all the Cu sites occupied by Fe atoms are equivalent, on average. There is no clear evidence for the presence of three doublets. Isomer shifts are in the range 0.23 to 0.25 mm s^{-1} in all cases. This shows that all Fe ions in the superconductor are in the Fe^{3+} charge state.

The inner doublet increases in intensity with time as well as with further heat treatment. Its intensity acquires a stable value after sufficient heat treatment. Its relative intensity also increases, almost linearly, as Fe content increases; from 30% for $x = 0.03$ to 50% for $x = 0.12$. The quadrupole splitting increases from 0.65 mm s^{-1} for $x = 0.03$ to 0.78 mm s^{-1} for $x = 0.12$. At low temperature this component splits magnetically. $H_{int}(4.2\ K) \approx 425$ kG which shows that these ions are in a high-spin Fe^{3+} state. These ions appear to have octahedral coordination of oxygen ions. The other doublet also changes with x. Its splitting increases from 1.73 to 1.84 mm s^{-1} as x increases from 0.03 to 0.12. H_{int} (4.2 K) $\approx$ 373 kG for these ions. These ions appear to be in low-spin states. Crystal field considerations suggest that these Fe^{3+} ions with low-spin configurations occur at the sites with square pyramidal configuration.

The magnetic ordering at lower temperatures has not shown signs of spin relaxation effects, though lines are broad. Spin glass ordering of Fe ions coexists with superconductivity.

References

[1] Lyubutin I S, Terziev V G, Smirnovkaya E M and Shapiro A Ya 1990 *Physica* C **169** 361
[2] Bhargava S C, Sharma R, Chakrabarty J S, Tomy C V and Malik S K 1991 *Bull. Mater. Sci.* **14** 675
[3] Eibschutz M, Lines M E and Tarascon J M 1988 *Phys. Rev.* B **38** 8858
[4] Felner I, Nowik I, Yaron U, Bauminger E R and Hechel D 1991 *Physica* C **185–9** 1117

[5] Tarascon J M, LePage Y, McKinnon W R, Ramesh R, Eibschutz M, Tselepis E, Wang E and Hull G W 1990 *Physica* C **167** 20–34
[6] Okada T, Kobayashi Y, Asai K, Yamada N and Yamadaya T 1991 *Physica* C **185–9** 1125
[7] Bhargava S C, Chakrabarty J S, Sharma R, Tomy C V and Malik S K 1990 *Solid State Commun.* **76** 1209
[8] Sinnemann Th, Job R and Rosenberg M 1992 *Phys. Rev.* B **45** 4941
[9] Morrish A H, Zhou X Z, Luo L Y, Li Z W and Maartense I 1990 *Hyperfine Interact.* **55** 1343
[10] Barb D, Diamandescu L, Tarina D, Aldica G and Cruceanu E 1990 *Hyperfine Interact.* **55** 1183
[11] Bremert O, Michaelsen C and Krebs H U 1989 *J. Appl. Phys.* **65** 1018
[12] Micklitz H, Zimmermann W, Moshchalkov V and Leonjuk L 1990 *Solid State Commun.* **75** 995
[13] Tittonen I, Hietaniemi J, Huttunen J, Linden J, Katila T, Karlemo T, Karppinen M, Niinisto L and Ullakkio K 1990 *Phys. Rev.* B **42** 4212
[14] Lin S T, Chung W S, Chou C Y and Lin C M 1990 *J. Phys.: Condens. Matter* **2** 8673
[15] Azad S, Gorochev O, Dormann J L, Sayouri S, Pankowska H and Suryanarayana R 1990 *J. Less-Common Met.* **164–5** 588
[16] Nowik I, Felner I and Bauminger E R 1992 *Phys. Rev.* B **45** 4912
[17] Kambe S, Matsuoka T, Takahasi M and Kawai M 1990 *Phys. Rev.* B **42** 2669
[18] Wange N H, Wang C M, Kao H C I, Ling D C, Ku H C and Lii K H 1989 *Japan. J. Appl. Phys.* **28** L1505
[19] Agarwal S K, Awana V P S, Moorthy V N, Maruthi Kumar P, Kumaraswamy B V, Narsimha Rao C V and Narlikar A V 1990 *Physica* C **160** 278
[20] Bhargava S C, Chakrabarty J S, Sharma R, Tomy C V and Malik S K 1991 *Solid State Commun.* **78** 397
[21] Roth G, Hager G, Renker B, Pannetier J, Caignaert V, Hervieu H and Raveau B 1988 *Z. Phys.* B **71** 43
[22] Bordet P, Hodeau J L, Strobel P, Marezio M and Santoro A 1988 *Solid State Commun.* **66** 435
[23] Krekels T, Van Tendeloo G, Broddin D, Amelincks S, Tanner L, Mehbod M, Vanlathem E and Deltour R 1991 *Physica* C **173** 361
[24] Trounov V A, Kaganovich T Yu, Kurbakov A I, Matveev A V, Balagurov A M, Hewat A W, Fischer P, Antson O and Maayouf R M A 1992 *Physica* C **197** 123
[25] Caignaert V, Maignan A and Raveau B 1991 *Physica* C **182** 219
[26] Koizumi A, Maeda H, Bamba N, Maruyama H, Takayama-Muromachi E, Jun Shi, Shimizu K, Mino M and Yamazaki Y 1989 *Japan. J. Appl. Phys.* **28** L203
[27] Boyce J B, Bridges F, Claeson T, Howland R S, Geballe T H and Nyaren M 1988 *Physica* C **153–5** 852
[28] Oyanagi H, Obara H, Yamaguchi H, Murata K, Ihara H, Matsushita T, Tokumoto M, Nishihara Y and Kimura Y 1989 *J. Phys. Soc. Japan* **58** 2140
[29] Kondo J, Asai Y and Nagai S 1988 *J. Phys. Soc. Japan* **57** 4334
[30] Howland R S, Geballe T H, Laderman S S, Fishercolbrie A, Scott M, Tarascon J M and Barbous P 1989 *Phys. Rev.* B **39** 9017
[31] Boekholt M, Bollmeier Th, Buschmann L, Fleuster M and Guntherodt G 1992 *Physica* C **198** 33
[32] Maeda A, Yabe T, Takebayashi S, Hase M and Uchinokura K 1990 *Phys. Rev.* B **41** 4112
[33] Mehbod M, Vanlathem W, Deltour R, Duvigneaud P H, Wyder P, Verwerft M, Van Tendeloo G and Van Landuyl J 1990 *Physica* C **168** 265
[34] Kulkarni P, Kulkarni S K, Nigavekar A S, Agarwal S K, Awana V P S and Narlikar A V 1990 *Physica* C **166** 530
[35] Yamagata S, Adachi K, Onada M, Fujishita H, Sera M, Ando Y and Sato M 1990 *Solid State Commun.* **74** 177
[36] Bauminger E R, Kowitt M, Felner I and Nowik I 1988 *Solid State Commun.* **65** 123
[37] Oashi T, Kumagai K, Nakajima Y, Tomita T and Fujita T 1989 *Physica* C **157** 315
[38] Lines M E and Eibschutz M 1990 *Physica* C **166** 235
[39] Bhargava S C, Sequeira A S, Chakrabarty J S, Rajagopal H, Sinha S K, Tomy C V and Malik S K 1992 *Solid State Commun.* **81** 1000
[40] Cava R J, Hewat A W, Hewat E A, Batlogg B, Marezio M, Rabe K M, Krajewski J J, Peck W F Jr and Rupp L W Jr 1990 *Physica* C **165** 419
[41] Beskrovnyi A I, Dlouha M, Jirak Z, Vratislav S and Pollert P 1990 *Physica* C **166** 79
[42] Vanlathem E, Mehbod M, Deltour R, Hennion M, Mirebeau I and Coddens G 1990 *Physica* C **185–9** 1171
[43] Vanlathem E, Mehbod M, Deltour R, Hennion M, Mirebeau I and Coddens G 1991 *Physica* C **177** 207